Inorg. Chem. **2004**, *43*, 2392–2401

A Thiazole-containing Tripodal Ligand: Synthesis, Characterization, and Interactions with Metal Ions and Matrix Metalloproteinases

Hongshan He,[†] Douglas P. Linder,[†] Kenton R. Rodgers,*[,†] Indrani Chakraborty,[†] and Atta M. Arif[‡]

Department of Chemistry, North Dakota State University, Fargo, North Dakota 58105-5516, and Department of Chemistry, University of Utah, Salt Lake City, Utah 84112-0850

Received July 12, 2003

A new tripodal ligand, tris[2-(((2-thiazolyl)methylidene)amino)ethyl]amine (Tatren), has been synthesized and characterized by NMR, IR, and UV–visible absorbance spectroscopy and elemental analysis. Tatren forms stable complexes with transition metal ions (Zn^{2+}, **1**; Mn^{2+}, **2**; Co^{2+}, **3**) and the alkaline earth metal ions (Ca^{2+}, **4**; Mg^{2+}, **5**). Single-crystal X-ray structures of **1**, **2**, and **5** revealed six-coordinate chelate complexes with formula $[M(Tatren)](ClO_4)_2$ in which the metal centers are coordinated by three thiazolyl N atoms and three acyclic imine N atoms. Crystals of **1**, **2**, and **5** are monoclinic, $P2_1/c$ space group. Crystals of **4** are triclinic, $P\bar{1}$ space group. The Ca^{2+} complex is eight-coordinate with all N atoms of Tatren and one water molecule coordinated to the metal ion. Spectrophotometric titrations show that formation constants for the chelates of metal ions are $\gg 1$ in methanol. Free Tatren inhibits the catalytic domain of matrix metalloproteinase-13 (MMP-13, collagenase-3) with $K_i = 3.5 \pm 0.6\ \mu$M. Molecular mechanics-based docking calculations suggest that one leg of Tatren coordinates to the catalytic Zn^{2+} in MMPs-2, -9, and -13 with significant hydrogen bonding to backbone amide groups. High-level DFT calculations suggest that, in the absence of nonbonded interactions between Tatren and the enzyme, the most stable first coordination sphere of the catalytic Zn^{2+} is achieved with three imidazolyl groups from His residues and two imine N atoms from one leg of Tatren. While complexes (**1**–**3**) do not inhibit MMP-13 to a significant extent, **4** does ($K_i = 30 \pm 10\ \mu$M). Hence, this study shows that tripodal chelating ligands of this class and their Ca^{2+} complexes have potential as active-site inhibitors for MMPs.

Introduction

Matrix metalloproteinases (MMPs) are a class of structurally related zinc-containing endopeptidases comprising more than 20 mammalian MMPs. They are classified into four subgroups on the basis of substrate specificity and domain structure, the collagenases, the stromelysins, the gelatinases, and the membrane-type MMPs. These enzymes play important roles in degradation and remodeling of the extracellular matrix.[1] However certain pathological conditions can cause imbalance in the activities of MMPs, which can lead to the destruction of cartilage and bone in rheumatoid and osteoarthritis, tissue breakdown and remodeling during invasive tumor growth and tumor angiogenesis, degradation of myelin-basic protein, opening of the blood-brain barrier, and breakdown of connective tissue in periodontal disease.[1,2]

The MMP catalytic domains exhibit high sequence homology and structural similarity.[3] Each includes two structurally and mechanistically distinct Zn(II) centers. One is thought to stabilize the protein structure whereas the other is crucial for catalysis. Single-crystal X-ray structure and solution NMR studies show that this zinc ion is coordinated by three imidazolyl groups from histidine (His) residues and one water

* To whom correspondence should be addressed. E-mail: Kent.Rodgers@ndsu.nodak.edu. Voice: 701-231-8746. Fax: 701-231-8831.
[†] North Dakota State University.
[‡] University of Utah.

(1) (a) Whittaker, M.; Floyd, C. D.; Brown, P.; Gearing, A. J. *Chem. Rev.* **1999**, *99*, 2735. (b) Wada, C. K.; Holms, J. H.; Curtin, M. L.; Dai, Y. J.; Florjancic, A. S.; Garland, R. B.; Guo, Y.; Heyman, H. R.; Stacey, J. R.; Steinman, D. H.; Albert, D. H.; Bouska, J. J.; Elmore, I. N.; Goodfellow, C. L.; Marcotte, P. A.; Tapang, P.; Morgan, D. W.; Michaelides, M. R.; Davidsen, S. K. *J. Med. Chem.* **2002**, *45*, 219. (c) Kotra, L. P.; Cross, J. B.; Shimura, Y.; Fridman, R.; Schlegel, H. B.; Mobashery, S. *J. Am. Chem. Soc.* **2001**, *123*, 3108.

(2) (a) Chambers, A. F.; Matrisian, L. M. *J. Natl. Cancer Inst.* **1997**, *89*, 1260. (b) Gijbels, K.; Masure, S.; Carton, H.; Opdenakker, G. *J. Neuroimmunol.* **1992**, *41*, 29. (c) Chandler, S.; Coates, R.; Gearing, A.; Lury, J.; Wells, G.; Bone, E. *Neurosci. Lett.* **1995**, *201*, 223.

(3) (a) Liotta, L. A.; Tryggvason, K.; Garbisa, S.; Robey, P. G.; Abe, S. *Biochemistry* **1981**, *20*, 100. (b) Wilhelm, S. M.; Collier, I. E.; Marmer, B. L.; Eisen, A. Z.; Grant, G. A.; Goldberg, G. I. *J. Biol. Chem.* **1989**, *264*, 17213. (c) Brown, D. L.; Hibbs, M. S.; Kearney, M.; Loushin, C.; Isner, J. M. *Circulation* **1995**, *91*, 2125.

10.1021/ic034811q CCC: $27.50
Published on Web 03/11/2004

molecule in the activated enzymes.[4] A recently published report suggests that three water molecules may be present.[5] Probably the most common aspect of MMP inhibition is the blocking of access to the catalytic Zn^{2+} through coordination or chelation by synthetic inhibitors. Some naturally occurring macromolecules, the tissue inhibitors of matrix metalloproteinases (TIMPs), also inhibit catalysis in part by blocking access to the catalytic Zn^{2+}.[1,6]

Many MMP inhibitors have been synthesized to date, and a large fraction of them are hydroxamic acid, carboxylic acid, thiol, and phosphorus derivatives.[7] Many are strong, competitive inhibitors (small K_i). The gross topology of tightly binding inhibitors is shown in Chart 1. In general, four groups are tethered to the inhibitor backbone. One is the zinc binding group (ZBG) which serves to chelate the catalytic zinc ion when these inhibitors are bound in the MMP active site. The R_1, R_2, and R_3 groups determine MMP selectivity, bioavailability, and affinity.[1] These groups have been systematically modified on a number of backbone scaffolds to improve both affinity and specificity for particular MMPs. Despite the vast amount of effort directed toward optimizing MMP inhibitors, only one has gained FDA approval and it is only for topical application. In general, these compounds bring about toxic side effects that make them ineffectual as pharmaceutical agents. Yet, the MMPs remain attractive therapeutic targets in the treatment of numerous disease states. Hence, there remains a need for the design and synthesis of effective MMP inhibitors with diminished toxicities for the treatment of the aforementioned diseases and disorders.

Many of the most tightly binding inhibitors have structural topologies reminiscent of tripodal chelating ligands. Specifically, they contain a ZBG and several other functionalities that facilitate nonbonded (H bonding and hydrophobic) interactions with the enzyme's substrate binding cleft. Thus,

Chart 1. Cartoon Illustrating Multiple Groups of Synthetic MMP Inhibitors, Which Interact with Binding Sites in and around the Active Sites of the Enzymes[a]

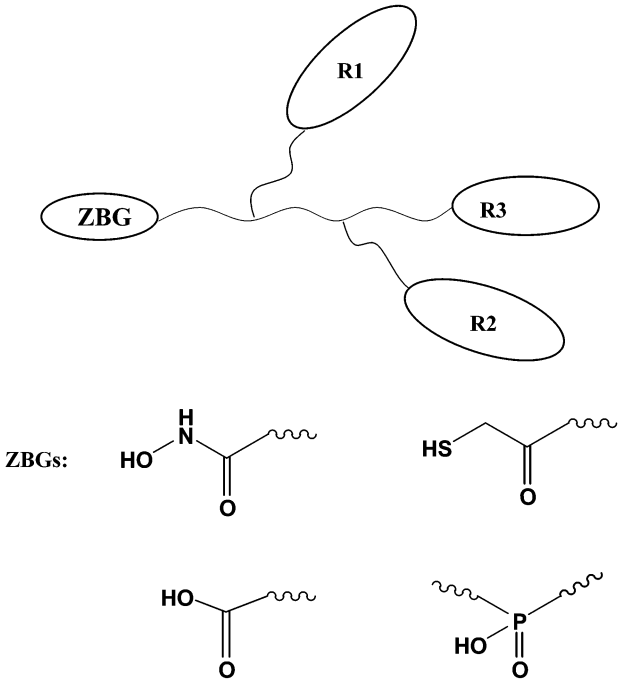

[a] Some common zinc binding groups are also shown.

we have undertaken a study of a new tris(2-aminoethyl)-amine-based chelating ligand as an MMP inhibitor because of its ability to chelate metal ions[8,9] and because it holds the possibility for forming multiple nonbonded interactions with the substrate binding cleft.

Herein, we report the synthesis and characterization of tris[2-(((2-thiazolyl)methylidene)amino)ethyl]amine. This ligand chelates transition and main-group metal ions in organic solvents, forming stable six- and eight-coordinate complexes (Chart 2). We further show that Tatren inhibits MMP-13 (collagenase 3) in water with $K_i = 3.5 \pm 0.6\ \mu M$. On the basis of competitive inhibition, molecular mechanics-based docking calculations, and high-level DFT calculations,

(4) (a) Roswell, S.; Hawtin, P.; Minshull, C. A.; Jepson, H.; Brockbank, S. M. V.; Barratt, D. G.; Slater, A. M.; McPheat, W. L.; Waterson, D.; Henney, A. M.; Pauptit, R. A. *J. Mol. Biol.* **2002**, *319*, 173. (b) Morgunova, E.; Tuuttila, A.; Bergmann, U.; Isupov, M.; Lindqvist, Y.; Schneider, G.; Tryggvason, K. *Science* **1999**, *284*, 1667. (c) Botos, I.; Meyer, E.; Swanson, S. M.; Lemmaitre, V.; Eechout, Y.; Meyer, E. F. *J. Mol. Biol.* **1999**, *292*, 837. (d) Pavlovsky, A. G.; William, M. G.; Ye, Q. Z. Ortwine, D. F.; Purchase, C. F., II; White, A. D.; Dhanaraj, V.; Roth, B. D.; Johnson, L. L.; Hupe, D.; Humblet, C.; Blundell, T. L. *Protein Sci.* **1999**, *8*, 1455. (e) Grams, F.; Crimmin, M.; Hinnes, L.; Huxley, P.; Pieper, M.; Tschesche, H.; Bode, W. *Biochemistry* **1995**, *34*, 14012.

(5) Bertini, I.; Calderone, V.; Fragai, M.; Luchinat, C.; Mngani, S.; Terni, B. *Angew. Chem., Int. Ed.* **2003**, *42*, 2673.

(6) Gomis-Ruth, F. X.; Maskos, K.; Betz, M.; Bergner, A.; Huber, R.; Suzuki, K.; Yoshida, N.; Nagase, H.; Brew, K.; Bourenkov, G. P.; Bartunik, H.; Bode, W. *Nature* **1997**, *389*, 77.

(7) (a) Puerta, D. T.; Cohen, S. M. *Inorg. Chem.* **2003**, *42*, 3423. (b) Puerta, D. T.; Cohen, S. M. *Inorg. Chem.* **2002**, *41*, 5075. (c) Hanessian, S.; Moitessier, N.; Cantin, L. D. *Tetrahedron* **2001**, *57*, 6885. (d) Hanessian, S.; Mackay, D. B.; Moitessier, N. *J. Med. Chem.* **2001**, *44*, 3074. (e) Jacobson, I. C.; Reddy, P. G.; Wasserman, Z. Z.; Hardman, K. D.; Covington, M. B.; Arner, E. C.; Copeland, R. A.; Decicco, C. P.; Magolda, R. L. *Bioorg. Med. Chem. Lett.* **1998**, *8*, 837. (f) Gowravaram, M. R.; Tomczuk, B. E.; Johnson, J. S.; Delecki, D.; Cook, E. R.; Ghose, A. K.; Mathiowetz, A. M.; Spurlino, J. C.; Rubin, B.; Smith, D. L. *J. Med. Chem.* **1995**, *38*, 2570. (g) Beszant, B.; Bird, J.; Gaster, L. M.; Harper, G. P.; Hughes, I.; Karran, E. H.; Markwell, R. E.; Miles-Willams, A. J.; Smith, S. A. *J. Med. Chem.* **1993**, *36*, 4030. (h) Bird, J.; De Mello, R. C.; Harper, G. P.; Hunter, D. J.; Karren, E. H.; Markwell, R. E.; Miles-Willams, A. J.; Rahman, S. S.; Ward, R. W. *J. Med. Chem.* **1994**, *37*, 158.

(8) (a) Schrock, R. R. *Acc. Chem. Res.* **1997**, *30*, 9. (b) Gade, L. H. *Acc. Chem. Res.* **2002**, *35*, 575. (c) Kol, M.; Schrock, R. R.; Kempe, R.; Davis, W. M. *J. Am. Chem. Soc*. **1994**, *116*, 4382.

(9) (a) Schatz, M.; Becher, M.; Walter, O.; Liehr, G.; Schindler, S. *Inorg. Chim. Acta* **2001**, *324*, 173. (b) Thaler, F.; Hampel, F.; Schinder, S.; Jacobson, R. R.; Tyeklar, Z.; Murthy, N. N.; Ghosh, P.; Chen, Q.; Zubieta, J.; Karlin, K. D. *Inorg. Chem.* **2001**, *40*, 2312. (c) Brewer, C. T.; Brewer, G.; Shang, M. Y.; Scheidt, W. R.; Muller, I. *Inorg. Chim. Acta* **1998**, *278*, 197. (d) Su, C. Y.; Yang, S. P.; Kang, B. S.; Mak, T. C. W. *Angew. Chem., Int. Ed.* **2001**, *40*, 1725. (e) Yang, S. P.; Zhu, H. L.; Yin, X. H.; Chen, X. M.; Ji, L. N. *Polyhedron* **2000**, *19*, 2237. (f) Morgenstern-Badarau, I.; Lambert, F.; Deroche, A.; Cesario, M.; Guilhem, J.; Keita, B.; Nadjo, L. *Inorg. Chim. Acta* **1998**, *275*−*276*, 234. (g) Katsuki, I.; Matsumoto, N.; Kojima, M. *Inorg. Chem.* **2000**, *39*, 3350. (h) Paul, S.; Barik, A. K.; Butcher, R. J.; Kar, S. K. *Polyhedron* **2000**, *19*, 2661. (i) Guo, S. H.; You, X. Z.; Yu, K. B.; Lu, J. P. *Inorg. Chem.* **1993**, *32*, 1883. (j) Chen, S.; Richardson, J. F.; Buchanan, R. M. *Inorg. Chem*. **1994**, *33*, 2376. (k) Wang, S. X.; Wang, L. F.; Wang, X. M.; Luo, Q. H. *Inorg. Chim. Acta* **1997**, *254*, 71. (l) Pascaly, M.; Duda, M.; Rompel, A.; Sift, B. H.; Meyer-Klaucke, W.; Krebs, B. *Inorg. Chim. Acta* **1999**, *291*, 289. (m) Sim, P. G.; Sinn, E. *Inorg. Chem.* **1978**, *17*, 1288. (n) Jantti, A.; Wagner, M.; Suontamo, R.; Kolehmainen, E.; Rissanen, K. *Eur. J. Inorg. Chem.* **1998**, 1555. (o) Jancsó, A.; Török, I.; Korecz, L.; Rockenbauer, A.; Gajda, T. *J. Chem. Soc., Dalton Trans*. **2002**, 2601. (p) Mohamadou, A.; Gerard, C. *J. Chem. Soc., Dalton Trans.* **2001**, 3320.

Chart 2. Tatren Ligand and the Metal Complexes Reported Herein

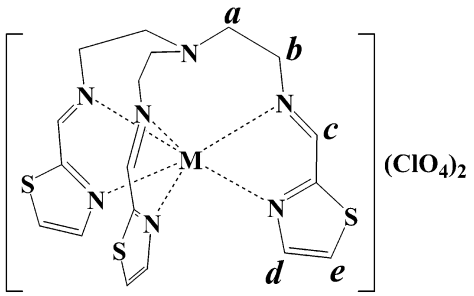

M^{2+}	Zn^{2+}	Mn^{2+}	Co^{2+}	Ca^{2+}	Mg^{2+}
$[M(Tatren)]^{2+}$	1	2	3	4*	5

* 8-coordinate, ternary amine N, and one OH_2 ligand bound.

we attribute this level of inhibition to the coordination of Tatren to the catalytic Zn^{2+} center. Finally, trans-metalation of the Ca^{2+} complex by Zn^{2+} suggests the possibility that alkaline earth metal ions could serve as in vivo carriers of MMP inhibitors based on this class of ligands.

Experimental Section

General Methods. All solvents were treated by standard methods prior to use. Reagent grade 2-thiazolecarboxaldehyde and tris(2-aminoethyl)amine (tren) were obtained commercially and used without further purification. Other chemicals were analytical grade and used as received. When necessary, the deionized water and buffers used in biological assay were passed over a column packed with chelating resin (Chelex 100). Elemental compositions were determined using a commercial C, H, and N analyzer. IR spectra were recorded from KBr pellets with a commercial FTIR spectrometer. ^{1}H and ^{13}C NMR spectra were acquired at 400 MHz in CD_3CN solution at 25 °C. UV−visible spectra were recorded with a commercial scanning spectrophotometer in a 1.0 cm quartz cell. MMP inhibition was quantified by a fluorescence-based assay using commercial instrument equipped with a reference detector and a photon-counting detection system.

Caution! *Perchlorate salts of compounds containing organic ligands can be extremely dangerous because of their propensity for explosive decomposition. Although we had no problems with explosion, only small quantities of these compounds should be prepared and they should be handled behind a protective shield. They should not be isolated by filtration using a sintered glass frit, and care should be taken to avoid heating and subjecting them to physical shock.*

[Zn(Tatren)](ClO$_4$)$_2$ (1). To a magnetically stirred solution of tren (0.146 g, 1.0 mmol) dissolved in 6 mL of freshly dried methanol was added 2-thiazolecarboxaldehyde (0.339 g, 3.0 mmol) dissolved in 4 mL of dried methanol. The solution was refluxed for 12 h, whereupon a 3-mL methanol solution containing 1.0 mmol of zinc acetate (0.300 g) and 1.0 mmol of sodium perchlorate (0.250 g) was added dropwise. The slight yellow solid precipitated immediately. The mixture was refluxed further for 2 h, and then the solid was collected by filtration using filter paper, washed with methanol, and dried under vacuum. Yield: 0.35 g, 51%. Mp: >200 °C. Anal. Calcd for $C_{18}H_{21}Cl_2N_7O_8S_3Zn$: C, 31.07; H, 3.04; N, 14.09. Found: C, 31.05; H, 2.84; N, 14.09. IR (KBr pellet): 3106 m, 2955 w, 2842 m, 2015 w, 1627 s, 1491 s, 1370 s, 1273 m, 1165 s, 1080 vs, 912 s cm^{-1}. ^{1}H NMR (CD_3CN, ppm): 8.71 (m, 3H, N═CH), 8.00 (d, J = 3.2, 3H, thiazolyl-H), 6.77 (dd, J^1 = 0.6, J^2 = 3.1 Hz, 3H, thiazolyl-H), 3.8 (broad, 3H, NCH_2), 3.6 (broad, 3H, NCH_2), 3.2 (broad, 3H, CH_2–N), 2.9 (broad, 3H, CH_2N). ^{13}C NMR (CD_3CN, ppm): 54.09, 56.13, 128.79, 141.87, 156.23, 161.95. UV−vis [CH_3CN, 25 °C; λ/nm (log ϵ)]: 289.4 (2.54), 234.2 (1.94).

[Mn(Tatren)](ClO$_4$)$_2$ (2). This complex was prepared as described for **1** except that manganous perchlorate hexahydrate (0.36 g) was used in place of the acetate salt and sodium perchlorate. Yield: 0.47 g, 71%. Mp: >200 °C. Anal. Calcd for $C_{18}H_{21}Cl_2MnN_7O_8S_3$: C, 31.54; H, 3.09; N, 14.30. Found: C, 31.59; H, 2.87; N, 14.42. IR (KBr pellet): 3118 m, 2959 w, 2854 w, 2019 w, 1623 s, 1487 s, 1374 s, 1277 m, 1165 s, 1099 vs, 912 m cm^{-1}. UV−vis [CH_3CN, 25 °C; λ/nm (log ϵ)]: 291.5 (2.83), 236.0 (2.10).

[Co(Tatren)](ClO$_4$)$_2$ (3). This complex was prepared as described for **1**. Cobalt acetate tetrahydrate (0.25 g) was used. Yield: 0.44 g, 65%. Mp: >200 °C. Anal. Calcd for $C_{18}H_{21}Cl_2CoN_7O_8S_3$: C, 31.36; H, 3.07; N, 14.22. Found: C, 31.34; H, 3.04; N, 14.30. IR (KBr pellet): 3118m, 3099m, 2918m, 2862m, 2011w, 1642s, 1405m, 1366s, 1281m, 1168s, 1085vs, 947s cm^{-1}. UV−vis [CH_3CN, 25 °C; λ/nm (log ϵ)]: 360.2 (1.86), 287.6 (2.85), 232.7 (2.25).

[Ca(Tatren)(H$_2$O)](ClO$_4$)$_2$ (4). This complex was prepared as described for **2**. Calcium perchlorate (0.24 g) was used. Yield: 0.47 g, 68%. Mp: >200 °C. Anal. Calcd for $C_{18}H_{23}CaCl_2N_7O_9S_3$: C, 31.40; H, 3.37; N, 14.24. Found: C, 31.53; H, 3.30; N, 14.24. IR (KBr pellet): 3426 m, 2989 m, 2940 m, 1603 s, 1490 s, 1362 s, 1280 m, 1102 vs, 780 m cm^{-1}. ^{1}H NMR (CD_3CN, ppm): 8.54 (t, J = 1.7 Hz, 3H, N═CH), 7.94 (m, 6H, thiazolyl-H), 3.91 (td, J^1 = 1.7 Hz, J^2 = 6.1 Hz, 6H, ═N−CH_2), 3.08 (t, J = 6.1 Hz, 6H, N−CH_2). ^{13}C NMR (CD_3CN, ppm): 54.30, 56.02, 128.65, 142.72, 156.80, 163.20. UV−vis [CH_3CN, 25 °C; λ/nm (log ϵ)]: 286.2 (2.48).

[Mg(Tatren)](ClO$_4$)$_2$ (5). This complex was prepared as described for **2**. Anhydrous magnesium perchlorate (0.22 g) was used. Yield: 0.51 g, 78%. Mp: >200 °C. Anal. Calcd for $C_{18}H_{21}Cl_2N_7MgO_8S_3$: C, 33.02; H, 3.23; N, 14.97. Found: C, 33.08; H, 3.14; N, 14.83. IR (KBr pellet): 3429 m, 2980 m, 2930 m, 1608 s, 1485 s, 1360 m, 1280 s, 1160 s, 1108 vs cm^{-1}. ^{1}H NMR (CD_3CN, ppm): 8.67 (d, J = 0.4 Hz, 3H, N═CH), 7.97 (d, J = 3.2 Hz, 3H, thiazolyl-H), 6.79 (d, J^1 = 0.4 Hz, J^2 = 3.2 Hz, 3H, thiazolyl-H), 3.82 (broad, 3H, N−CH_2), 3.55 (broad, 3H, N−CH_2), 3.07 (broad, 3H, CH_2–N), 2.91 (broad, 3H, CH_2–N). ^{13}C NMR (CD_3CN, ppm): 54.25, 56.00, 128.38, 142.36, 157.4, 163.14. UV−vis [CH_3CN, 25 °C; λ/nm (log ϵ)]: 287.5 (2.40).

Preparation of Tatren. The Tatren ligand was prepared by demetalation of its Mn^{2+} complex in the presence of base. To a solution of **2** (0.40 g) in 20 mL of methanol was added 5.0 mL of 10% aqueous sodium hydroxide, and the mixture was stirred magnetically at room temperature for 15 min. The solution was filtered, and the filtrate was extracted with chloroform (3 × 20 mL); the combined organic mixture was washed three times with water. After the solvent was removed and dried under vacuum, a slightly yellow oil was obtained. Yield: 0.22 g, 88%. Anal. Calcd for $C_{18}H_{21}N_7S_3$: C, 50.09; H, 4.90; N, 22.72. Found: C, 49.61; H, 4.79; N, 22.24. IR (KBr pellet): 3083 m, 2951 m, 2893 m, 2838 m, 1638 s, 1483 s, 1421 m, 1355 s, 1231 m, 1149 s, 939 m, 788 m, 699 m cm^{-1}. ^{1}H NMR (CH_3CN, ppm): 8.38 (tt, J^1 = 1.3 Hz J^2 = 1.3 3H, N═CH), 7.87 (dd, J^1 = 1.2 Hz J^2 = 3.2 Hz, 3H, thiazole), 7.51 (dt, J^1 = 2.3 Hz J^2 = 3.2 Hz, 3H, thiazole), 3.70 (tt, J^1 = 1.2 Hz J^2 = 6.4 Hz, 6H, N−CH_2), 2.91 (td, J^1 = 1.2 Hz J^2 = 6.4, 6H, CH_2–N). ^{13}C NMR ($CDCl_3$, ppm): 55.38, 59.97, 121.68, 144.15, 156.06, 165.20. UV−vis [CH_3CN, 25 °C; λ/nm (log ϵ)]: 285.2 (2.40).

Table 1. Crystallographic Data Collection and Refinement Parameters for **1**, **2**, **4**, and **5**

	1	**2**	**4**	**5**
formula	$C_{36}H_{42}Cl_4Zn_2N_{14}O_{16}S_6$	$C_{18}H_{21}Cl_2MnN_7O_8S_3$	$C_{18}H_{23}CaCl_2N_7O_9S_3$	$C_{18}H_{21}Cl_2MgN_7O_8S_3$
fw	1391.74	685.44	688.59	654.81
system	monoclinic	monoclinic	triclinic	monoclinic
space group	$P2_1/c$	$P2_1/c$	$P\bar{1}$	$P2_1/c$
temp (K)	297(2)	300(2)	150(1)	150(1)
a (Å)	16.5672(13)	16.6871(14)	9.4379(2)	16.5444(4)
b (Å)	9.0227(7)	9.0292(8)	10.0327(3)	8.90900(1)
c (Å)	18.0083(14)	17.9807(15)	15.5197(4)	17.8894(5)
α (deg)	90	90	87.8463(13)	90
β (deg)	95.3430(10)	95.135(2)	82.3860(15)	95.3245(11)
γ (deg)	90	90	70.7546(14)	90
V (Å^3)	2680.2(4)	2698.3(4)	1375.14(6)	2625.41(10)
Z	2	4	2	4
D_{calcd} (g·cm^{-3})	1.725	1.687	1.663	1.657
F(000)	1416	1396	708	1344
μ (mm^{-1})	1.407	0.977	0.712	0.569
reflcns collcd	15 956	19 217	9661	10 664
indpndnt reflcns	6138	6238	6228	5997
data/params	6138/352	6238/352	6228/454	5997/436
GOF on F^2	0.935	1.046	1.030	1.041
final R indices ($I > 2\sigma$)	R1 = 0.0355	R1 = 0.0555	R1 = 0.0359	R1 = 0.0349
	wR2 = 0.0968	wR2 = 0.1569	wR2 = 0.0872	wR2 = 0.0813
R indices (all data)	R1 = 0.0552	R1 = 0.0805	R1 = 0.0451	R1 = 0.0484
	wR2 = 0.1015	wR2 = 0.1726	wR2 = 0.0933	wR2 = 0.0889

X-ray Crystallographic Analysis of [Zn(Tatren)](ClO$_4$)$_2$ and [Mn(Tatren)](ClO$_4$)$_2$. Single crystals of **1** and **2** were obtained by slow evaporation of solvent from the respective complexes in ~1:1 (v:v) mixtures of methanol and acetonitrile at room temperature. The crystals were mounted on glass fibers before data collection. The crystals were stable in air so no effort was made to protect them from the laboratory atmosphere. Diffraction measurements were made on a CCD-based commercial X-ray diffractometer using Mo Kα radiation (λ = 0.710 73 Å). The frames were collected at ambient temperature with a scan width 0.3° in ω and intergrated with Brucker SAINT software package using narrow-frame integration algorithm. The unit cell was determined and refined by least-squares upon the refinement of *XYZ*-centeroids of reflections above 20σ(*I*). The data were corrected for absorption using SADABS program. The structures were refined on F^2 using the Bruker SHELXTL (version 5.1) software package.

X-ray Crystallographic Analysis of [Ca(Tatren)(OH$_2$)](ClO$_4$)$_2$ and [Mg(Tatren)](ClO$_4$)$_2$. Colorless prisms (**4**) and plate-shaped (**5**) crystals were obtained as described in the previous section, mounted on glass fibers with traces of viscous oil, and then transferred to a commercial CCD-based diffractometer using Mo Kα radiation (λ = 0.710 73 Å). A total of 10 frames of data were collected at 150(1) K with an oscillation range of 1°/frame and an exposure time of 20 s/frame.[10] Indexing and unit cell refinement was based on all observed reflections from those 10 frames, indicated a triclinic *P* lattice. Reflections were indexed, integrated, and corrected for Lorentz, polarization, and absorption effects using DENZO-SMN and SCALEPAC.[11]

The structures were solved by a combination of direct methods and heavy atom using SIR 97.[12] All of the non-hydrogen atoms were refined with anisotropic displacement coefficients. Hydrogen atoms were located and refined isotropically using SHELXL97.[13] The weighting scheme employed was $w = 1/[\sigma^2(F_o^2) + (0.0386P)^2 + 1.2965P]$, where $P = (F_o^2 + 2F_c^2)/3$.[14] The refinements converged to parameters indicated in Table 1. The maximum Δ/σ in the final cycles of the least-squares was 0.001, and the residual peaks on the final difference Fourier maps are as indicated in Table 1. Scattering factors were taken from refs 15 and 16. Crystallographic and structure refinement parameters are listed in Table 1.

Spectrophotometric and NMR Titrations. Spectrophotometric titrations of Tatren by metal ions were carried out with a scanning UV−visible spectrophotometer equipped with a temperature-controlled cell block. A 3.0-mL solution of Tatren in methanol (3.615×10^{-5} M) was titrated with a methanolic solution of the respective metal perchlorate. Additions were made to a septum-sealed 1.0 cm cuvette (to minimize evaporation) using a 10-μL syringe. The resulting solution was stirred magnetically for 15 min to ensure that equilibrium had been established before the spectra were recorded. The total increase in volume was less than 0.5%.

Trans-metalation reactions were carried out in titration style by adding 5-μL aliquots of an acetonitrile-d_3 solution of Zn(ClO$_4$)$_2$·6H$_2$O to a solution of [Ca(Tatren)(OH$_2$)](ClO$_4$)$_2$ in methanol. The extent of reaction was tracked by recording the 400-MHz ^{1}H NMR spectrum after each addition of zinc.

MMP Assay. Catalytic domain of mouse MMP-13 was prepared by literature method[4c] using BL21/DE3 *Escherichia coli* as expresser and purified using HPLC with gradient elution from a DEAE ion exchange column. Purity and molecular weight (kDa) were determined by SDS−PAGE. Inhibition of MMP-13 was quantified by using the OmniMMP Mca-Pro-Leu-Gly-Leu-Dpa-

(10) *COLLECT Data Collection Software*; Nonius, BV: Delft, The Netherlands, 1998.
(11) Otwinowski, Z.; Minor, W. *Methods Enzymol.* **1997**, *276*, 307−326.
(12) Altomare, A.; Burla, M. C.; Camalli, M.; Cascarano, G.; Giacovazzo, C.; Guagliardi, A.; Moliteni, A. G. G.; Polidori, G.; Spagna, R. SIR97 (Release 1.02)-A program for automatic solution and refinement of crystal structure.
(13) SHELX97 (includes SHELXS97, SHELXL97, and CIFTAB): Sheldrick, G. M. *Programs for Crystal Structure Analysis (Release 97-2)*; University of Göttingen: Göttingen, Germany, 1997.
(14) R1 = $\Sigma(||F_o| - |F_c||)/\Sigma|F_o|$, wR2 = $[\Sigma(w(F_o^2 - F_c^2)^2)/\Sigma(F_o^2)^2]^{1/2}$, and S = goodness-of-fit on $F^2 = [\Sigma(w(F_o^2 - F_c^2)^2/(n - p)]^{1/2}$, where n is the number of reflections and p is the number of parameters refined.
(15) Maslen, E. N.; Fox, A. G.; O'Keefe, M. A. *International Tables for Crystallography: Mathematical, Physical and Chemical Tables*; Wilson, A. J. C., Ed.; Kluwer: Dordrecht, The Netherlands, 1992; Vol. C, Chapter 6, pp 476−516.
(16) Creagh, D. C.; McdAuley, W. J. *International Tables for Crystallography: Mathematical, Physical and Chemical Tables*; Wilson, A. J. C., Ed.; Kluwer: Dordrecht, The Netherlands, 1992; Vol. C, Chapter 4, pp 206−222.

Ala-Arg-NH_2AcOH as a fluorogenic substrate and Mca-Pro-Leu-OH as reference peptide (Mca = (7-methoxycoumarin-4-yl)acetyl and Dpa = *N*-3-(2,4-dinitrophenyl)-L-α, *β*-diaminopropionyl), as per published procedures.[17] All assays were carried out in Hepes buffer that was 100 mM in $CaCl_2$ and contained 0.05% Brij-35 at pH = 7.40 and 37 °C. The initial rates were measured by tracking the appearance of unquenched Mca fluorescence at 393 nm (λ_{exc} = 328 nm) for 5 min using a commercial spectrofluorometer. Typically, 50 μL of MMP-13 (15 nM) in buffer and 10 μL of inhibitor (10 μM) in DMSO were injected into 947 μL of buffer. After a 10-min incubation period the assay was initiated by addition of 3 μL of the fluorogenic substrate (10 μM). The inhibition constant, K_i, was calculated from the dependence of initial rates on initial concentration.[18]

Molecular Modeling. Docking calculations were performed using FlexX as implemented in the Sybyl 6.8 package.[19] FlexX uses an incremental construction algorithm to place ligands into a protein active site. To define the active site, we chose a radius of 8 Å around the original bound inhibitor in the X-ray structures of MMP-13 (PDB code: 830C),[20] MMP-9 (1GKC),[21] and MMP-3 (1D8F).[22] Where there was no inhibitor-bound X-ray structure available, MMP-2 (1QIB),[23] we chose as our active site the catalytic Zn atom with all residues having at least one atom within a 12-Å radius. The only other deviation from the FlexX default parameters was to place hydrogen atoms on the Nδ1 nitrogens of the imidazole rings coordinated to the zinc center, as indicated by the crystal structures. FlexX puts the proton on Nϵ2 by default. The docking calculations were performed using the free ligand, which was first minimized using the Tripos force field.

Higher level quantum chemical calculations were performed at the density functional theory (DFT) and semiempirical PM3 levels of theory on a portion of the Tatren-bound active site. Specifically, multiple structures were minimized at the PM3 level and B3LYP/6-31G levels of theory. These structures were subsequently verified as minima via force constant calculations. The PM3 calculations were performed using MOPAC 6.0 as implemented in Sybyl 6.8 while the B3LYP/6-31G calculations were performed using Gaussian 98.[24] To obtain a better estimate of the energetics, single point DFT, B3LYP/6-31G*, calculations were performed at the 6-31G stationary points, B3LYP/6-31G*//6-31G. Zero-point energy corrections and thermal effects at 298 K are included in the final relative energies.

Results and Discussion

Synthesis and Characterization of Tatren and Its Transition Metal Complexes. Reaction of 2-thiazolecarboxaldehyde with tren in methanol gave the tris(imine) product, Tatren. The resulting solution was treated with metal perchlorate salts to yield the respective hexacoordinate complexes. Attempts to isolate the Tatren ligand from the condensation reaction were unsuccessful. Consequently, Tatren was prepared by demetalation of the Mn^{2+} complex in strong base. Carbon, hydrogen, and nitrogen analyses of the solid complexes indicated the general formulas M(Tatren)-$(ClO_4)_2$ for M = Zn^{2+}, Mn^{2+}, and Co^{2+}. Lack of N−H stretching bands (3150−3450 cm^{-1}) in the FTIR spectrum of Tatren indicated that all three legs of tren had been functionalized. A strong band at about 1630 cm^{-1} is attributed to the formation of a C═N bond. Detailed structural information was obtained from single-crystal diffraction studies.

Crystals of **1** (001.cif) and **2** (002.cif) grew as thin plates. Both complexes crystalized as monoclinic with space group $P2_1/c$, and their structures are similar. Figure 1 shows ORTEP projections of **1**, which reveal the hexacoordinate structure and the pseudo-C_3 "boat screw" symmetry of the complex. Selected bond distances and angles are listed in Table 2 for **1** and **2**. Six N atoms, three from thiazolyl groups and three from acyclic imine groups, coordinate to the central metal ion giving complexes with distorted octahedral coordination spheres. The structure of **2** is shown in Figure S1.

Table 2 shows that the angles between Zn−N_{Imine} bonds are substantially larger than 90° and those between Zn−$N_{Thiazolyl}$ bonds are slightly less than 90°. The consequence of these bond angle differences is that the Zn atom is closer to the imine-N plane than it is to the thiazole-N plane. This distortion from an octahedral structure is required to accommodate the planarity of the bidentate diimine moieties.

While the M−N bond lengths are typical, slight variation is observed among the bonds of a single complex ion. As Table 2 shows, the average M−N_{Imine} bond distance is shorter than that of its M−$N_{Thiazolyl}$ counterpart. For example, the average Zn−N_{Imine} bond distance is 2.147 Å, whereas the average Zn−$N_{Thiazolyl}$ bond length is 2.262 Å. The distance between the tertiary amine nitrogen, N(1), and Zn is 2.929 Å in **1**, suggesting a weak interaction. The plane formed by imine nitrogen atoms, N(2), N(4), and N(6), is almost parallel to that formed by thiazolyl nitrogen atoms, N(3), N(5), and N(7). The five-membered chelate ring involving the metal ion is planar and nearly parallel with the thiazole ring. The average dihedral angle between the chelate ring and the plane defined by the tertiary amine N, Zn, and the imine N atoms,

(17) Lemaître, V.; Jungbluth, A.; Eeckhout, Y. *Biochem. Biophys. Res. Commun.* **1997**, *230*, 202.
(18) Cantor, C. R.; Schimmel, P. R.; Freeman, W. H. *Biophysical Chemistry, Part III: The Behavior of Biological Macromolecules*; W. H. Freeman and Company: New York, 1980; Chapter 17.
(19) *SYBYL*, version 6.8; Tripos Inc.: St. Louis, MO, 2002.
(20) Lovejoy, B.; Welch, A. R.; Carr, S.; Luong, C.; Broka, C.; Hendricks, R. T.; Campbell, J. A.; Walker, K. A.; Martin, R.; Van Wart, H.; Browner, M. F. *Nat. Struct. Biol.* **1999**, *6*, 217.
(21) Rowsell, S.; Hawtin, P.; Minshull, C. A.; Jepson, H.; Brockbank, S.; Barratt, D.; Slater, A. M.; Mcpheat, W.; Waterson, D.; Henney, A.; Pauptit, R. A. *J. Mol. Biol.* **2002**, *319*, 173.
(22) Cheng, M. L.; De, B.; Pikul, S.; Almstead, N. G. Natchus, M. G.; Anastasio, M. V.; Mcphail, S. J. Snider, C. E.; Taiwo, Y. O.; Chen, L. Y.; Dunaway, M.; Gu, F.; Dowty, M. E.; Mieling, G. E.; Janusz, M. J.; Wang-Weigand, S. *J. Med. Chem.* **2000**, *43*, 369.
(23) Dhanaraj, V.; Willliams, M. G.; Ye, Q. Z.; Molina, F.; Johnson, L. L.; Ortwine, D. F.; Pavlovsky, A.; Rubin, J. R.; Skeean, R. W.; White, A. D.; Humblet, C.; Hupe, D. J.; Blundell, T. L. *Croat. Chem. Acta* **1999**, *72*, 575.
(24) Frisch, M. J.; Trucks, G. W.; Schlegel, H. B.; Scuseria, G. E.; Robb, M. A.; Cheeseman, J. R.; Zakrzewski, V. G.; Montgomery, J. A., Jr.; Stratmann, R. E.; Burant, J. C.; Dapprich, S.; Millam, J. M.; Daniels, A. D.; Kudin, K. N.; Strain, M. C.; Farkas, O.; Tomasi, J.; Barone, V.; Cossi, M.; Cammi, R.; Mennucci, B.; Pomelli, C.; Adamo, C.; Clifford, S.; Ochterski, J.; Petersson, G. A.; Ayala, P. Y.; Cui, Q.; Morokuma, K.; Rega, N.; Salvador, P.; Dannenberg, J. J.; Malick, D. K.; Rabuck, A. D.; Raghavachari, K.; Foresman, J. B.; Cioslowski, J.; Ortiz, J. V.; Baboul, A. G.; Stefanov, B. B.; Liu, G.; Liashenko, A.; Piskorz, P.; Komaromi, I.; Gomperts, R.; Martin, R. L.; Fox, D. J.; Keith, T.; Al-Laham, M. A.; Peng, C. Y.; Nanayakkara, A.; Challacombe, M.; Gill, P. M. W.; Johnson, B.; Chen, W.; Wong, M. W.; Andres, J. L.; Gonzalez, C.; Head-Gordon, M.; Replogle, E. S.; Pople, J. A. *Gaussian 98*, revision A.11.4; Gaussian, Inc.: Pittsburgh, PA, 2002.

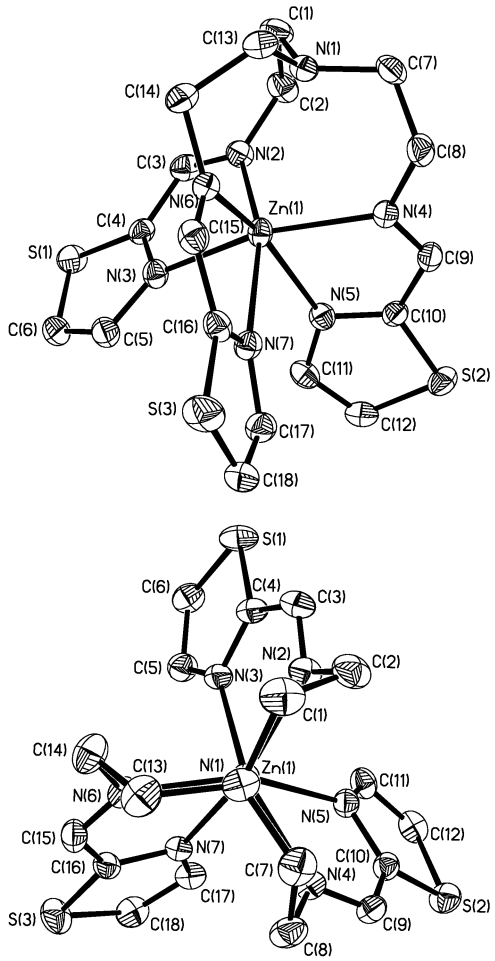

Figure 1. ORTEP diagrams for **1**, showing 30% probability ellipsoids: (top) side view; (bottom) view along C_3 symmetry axis, with Zn atom behind the apical N atom of Tatren. Hydrogen atoms and perchlorate counterions are omitted for clarity.

Table 2. Selected Bond Distances (Å) and Angles (deg) for **1** and **2**

bond	dist	bonds	angles
		Compound **1**	
Zn(1)−N(2)	2.136(2)	N(2)−Zn(1)−N(4)	102.52(8)
Zn(1)−N(4)	2.183(2)	N(6)−Zn(1)−N(2)	107.91(9)
Zn(1)−N(6)	2.121(2)	N(5)−Zn(1)−N(7)	81.19(8)
Zn(1)−N(3)	2.206(2)	N(2)−Zn(1)−N(3)	76.54(8)
Zn(1)−N(5)	2.283 (2)	N(6)−Zn(1)−N(7)	75.35(8)
Zn(1)−N(7)	2.300(2)	N(4)−Zn(1)−N(6)	100.18(8)
		N(3)−Zn(1)−N(5)	86.84(8)
		N(7)−Zn(1)−N(3)	85.10(8)
		N(4)−Zn(1)−N(5)	74.76(8)
		Compound **2**	
Mn(1)−N(2)	2.241(3)	N(2)−Mn(1)−N(4)	110.37(11)
Mn(1)−N(4)	2.229(3)	N(6)−Mn(1)−N(2)	104.43(10)
Mn(1)−N(6)	2.278(3)	N(5)−Mn(1)−N(7)	80.39(10)
Mn(1)−N(3)	2.306(3)	N(2)−Mn(1)−N(3)	72.61(10)
Mn(1)−N(5)	2.373(3)	N(6)−Mn(1)−N(7)	71.81(10)
Mn(1)−N(7)	2.353(3)	N(4)−Mn(1)−N(6)	101.95(10)
		N(3)−Mn(1)−N(5)	83.83(10)
		N(7)−Mn(1)−N(3)	86.22(10)
		N(4)−Mn(1)−N(5)	72.13(11)

N(1)−Zn(1)−N(4), is 148.13° for **1**. Although attempts to obtain diffraction quality crystals for the Co(II) complex were unsuccessful, elemental analysis, FTIR spectra, and UV−visible spectra suggest that the complex has a solution structure similar to those of **1** and **2**.

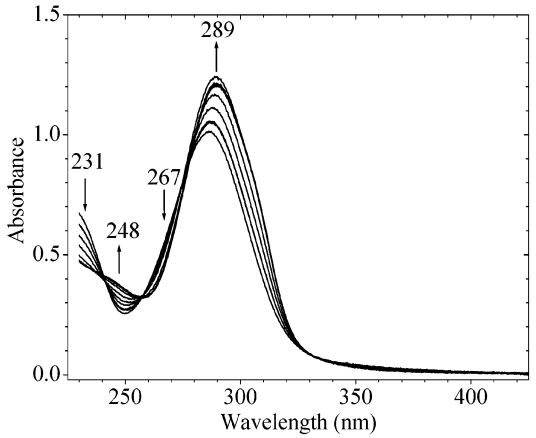

Figure 2. UV−visible spectral changes during titration of Tatren with 7.62×10^{-3} M Zn^{2+} in MeOH at room temperature. $[Tatren]_{final} = 3.615 \times 10^{-5}$ M; $[Zn^{2+}]_{final} = 3.80 \times 10^{-5}$ M.

A prominent, albeit common, structural feature of these tripodal ligand complexes is their chirality.[9h,25] The ORTEP diagram in Figure 1 shows a view of the **1** along the N(1)−M vector (pseudo-C_3 axis) and clearly shows the handedness of the cationic complex. However, both enantiomers are present in equal numbers in the unit cell of the crystal. Hence, the crystals grown under conditions reported here are racemic. Although, as has recently been reported,[9h,25b] it is possible to resolve such racemates by crystallization, our attempts to do so have been unsuccessful. One O atom of a perchlorate counterion is involved in a van der Waals interaction with the S atom of a thiazolyl group (O−S distance in **1** is 2.943 Å). However, no long-range network of these interactions is apparent from the packing diagram.

Interaction of Tatren with Transition Metal Ions in Solution. Tatren forms stable 1:1 complexes with transition metal ions in methanol solution. UV−visible spectrophotometric titration data for Zn^{2+}/Tatren and Co^{2+}/Tatren are shown in Figures 2, S3, and S4.

For the Zn^{2+} complex, absorbance at 286 nm increased and λ_{max} shifted to 289 nm, while absorbance decreased at 231 nm and increased at 248 nm. Another broad band centered at 360 nm was observed for $[Co(Tatren)]^{2+}$. Isosbestic points were observed at 238, 256, and 281 nm, and the final spectra of the titrations were identical with those obtained from solutions of the isolated complexes. When the concentration of the Zn^{2+} or Co^{2+} ion is greater than that of Tatren, the absorbance features of the complexes no longer change, as shown for the Co^{2+} titration in Figure S3. The Job's plot shown in Figure S4 reveals formation of a 1:1 complex for the Co^{2+} complex in methanol solution. Although the thermodynamic stabilities of these complexes

(25) (a) Nagasato, S.; Katsuki, I.; Motada, Y.; Sunatsuki, Y.; Matsumota, N.; Kojima, M. *Inorg. Chem.* **2001**, *40*, 2534. (b) Katsuki, I.; Motada, Y.; Sunatsuki, Y.; Matsumoto, N.; Nakashima, T.; Kojima, M. *J. Am. Chem. Soc.* **2002**, *124*, 629. (c) Miyasaka, H.; Okamura, S.; Nakashima, T.; Matsumoto, N. *Inorg. Chem.* **1997**, *36*, 4329. (d) Nagasato, S.; Sunatsuki, Y.; Ohsato, S.; Kido, T.; Matsumoto, N.; Kojima, M. *Chem. Commun.* **2002**, 14. (e) Katsuki, I.; Matsumoto, N.; Kojima, M. *Inorg. Chem.* **2000**, *39*, 3350. (f) Shii, Y.; Motoda, Y.; Matsuo, T.; Kai, F.; Nakashima, T.; Tuchagues, J.; Matsumoto, N. *Inorg. Chem.* **1999**, *38*, 3513.

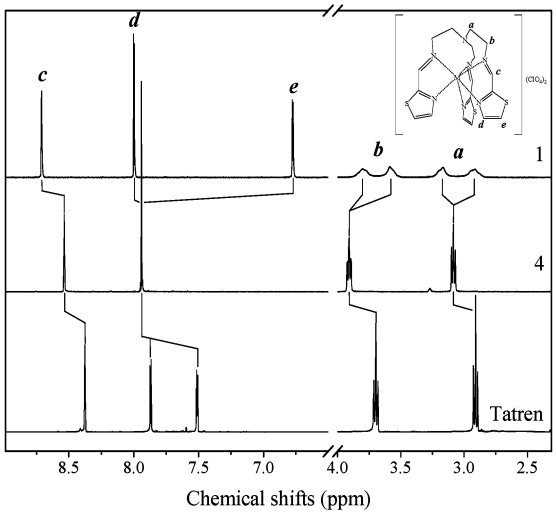

Figure 3. 400-MHz ^{1}H NMR spectra of Tatren, **1**, and **4** in CD_3CN.

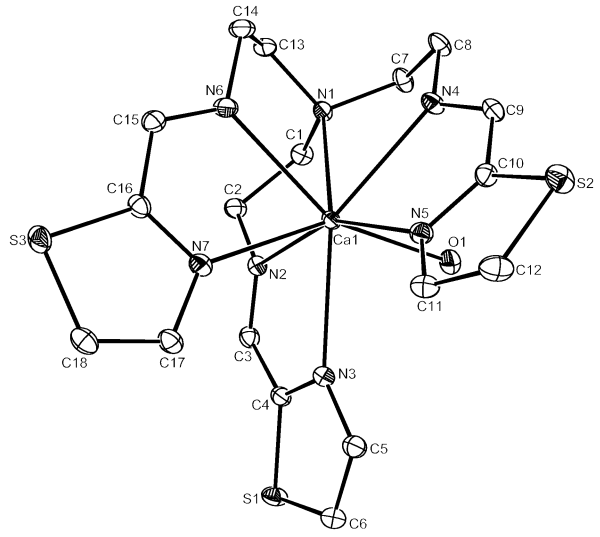

Figure 4. ORTEP rendering of the $[Ca(Tatren)(OH_2)](ClO_4)_2$ with 30% probability ellipsoids. Hydrogen atoms and perchlorate ions have been omitted for clarity. All seven nitrogen atoms of the Tatren ligand are within bonding distance of Ca^{2+}, and one water molecule is coordinated.

Table 3. Selected Bond Distances (Å) and Angles (deg) for **4** and **5**

bond	dist	bonds	angle
	Compound **4**		
Ca(1)−N(1)	2.6903(17)	N(2)−Ca(1)−N(4)	131.81(6)
Ca(1)−N(2)	2.4715(16)	N(6)−Ca(1)−N(2)	91.19(6)
Ca(1)−N(4)	2.5070(16)	N(5)−Ca(1)−N(7)	85.03(5)
Ca(1)−N(6)	2.5088(18)	N(2)−Ca(1)−N(3)	66.08(5)
Ca(1)−N(3)	2.5731(16)	N(6)−Ca(1)−N(7)	64.73(6)
Ca(1)−N(5)	2.5437 (17)	N(4)−Ca(1)−N(6)	83.08(6)
Ca(1)−N(7)	2.6143(17)	N(3)−Ca(1)−N(5)	90.87(5)
Ca(1)−O(1)	2.4368(17)	N(7)−Ca(1)−N(3)	75.20(5)
		N(4)−Ca(1)−N(5)	66.96(5)
		O(1)−Ca(1)−N(3)	73.13(6)
		O(1)−Ca(1)−N(5)	87.17(6)
		O(1)−Ca(1)−N(7)	147.22(6)
	Compound **5**		
Mg(1)−N(2)	2.1988(17)	N(2)−Mg(1)−N(4)	106.71(6)
Mg(1)−N(4)	2.1875(17)	N(6)−Mg(1)−N(2)	101.36(6
Mg(1)−N(6)	2.2231(17)	N(5)−Mg(1)−N(7)	83.04(6)
Mg(1)−N(3)	2.2020(17)	N(2)−Mg(1)−N(3)	75.62(6)
Mg(1)−N(5)	2.2434(16)	N(6)−Mg(1)−N(7)	74.65(6)
Mg(1)−N(7)	2.2527(17)	N(4)−Mg(1)−N(6)	99.274(6)
		N(3)−Mg(1)−N(5)	86.90(6)
		N(7)−Mg(1)−N(3)	88.44(6)
		N(4)−Mg(1)−N(5)	74.88(6)

were not determined, these titrations clearly show that Tatren effectively chelates the 2+ transition metal ions studied here with stability constants $\gg 1$.

The ^{1}H NMR spectrum of Tatren (Figure 3) contains five peaks, corresponding to the five proton environments of the ligand. Chemical shifts for the two methylene groups are 3.74 and 2.96 ppm for H^a and H^b respectively. Thiazolyl protons H^d and H^e give rise to the resonances at 7.36 and 7.86 ppm, respectively. Proton H^c gives rise to a singlet at 8.39 ppm. The general features of the Tatren ^{1}H NMR spectrum are preserved in spectra of the diamagnetic transition metal complexes. However, different metal ions have distinguishable effects on the ^{1}H chemical shifts of the Tatren protons and on the chemical shift pattern for the methylene protons. The thiazolyl resonances of **4** appear at 7.94 ppm, and the proton on the carbon atom bridging the imine nitrogen and the thiazole ring gives rise to a triplet at 8.54 ppm. Two triplets centered at 3.91 and 3.08 ppm arise from the methylene protons of **4**. In contrast, the spectra of **1** contains four unresolved multiplets centered at 3.80, 3.59, 3.17, and 2.91 ppm. The differences in the methylene regions of the spectra of **1** and **4** are due to differences in the conformational dynamics of the Tatren ligand. The chelate complexes are chiral, as seen by the bottom view of the structure in Figure 1. In this structure, the geminal methylene protons of Tatren are chemically inequivalent and, as such, have the distinct resonance frequencies revealed in the spectrum of **1** (Figure 3, top). Similar behavior has been observed for other ligands of this class.[26] The methylene region in the spectrum of **5** (not shown) also exhibits four broad resonances, each integrating for three protons. When the enantiomers are in rapid exchange on the NMR time scale, the spectrum contains average methylene proton resonances, as seen by the triplets in the spectrum of **4** (Figure 3, middle).

Complexes of Alkaline-Earth Metal Ions. Given the substantial in vivo concentrations of Mg^{2+} (1−3 mM) and Ca^{2+} (2.45 mM), any therapeutic application of a metal chelating agent must account for the interactions between the ligand and these alkaline-earth metal ions. Accordingly, the coordination chemistry of Tatren with Mg^{2+} and Ca^{2+} has been investigated. With Mg^{2+}, a stable 1:1 complex of formula $[Mg(Tatren)](ClO_4)_2$ (**5**, 005.cif) forms with a structure analogous to those of **1** and **2** (Figure S2). Figure 4 shows that, consistent with its large size, the Ca^{2+} complex (**4**, 004.cif) is octacoordinate with one water molecule coordinated between two legs of the Tatren ligand and a bond between Ca^{2+} and the tertiary nitrogen atom of Tatren (Table 3). In the crystal, two complexes are bridged by a hydrogen bond network involving the coordinated water molecules as hydrogen bond donors and the perchlorate counterions as acceptors. Both of these alkaline-earth complexes are stable in solution. The ^{1}H NMR spectrum of **5** is similar to that of **1** in Figure 3. Thorough solution characterization of these complexes will be reported elsewhere.

(26) He, H. S.; Rodgers, K. R. Submitted for publication.

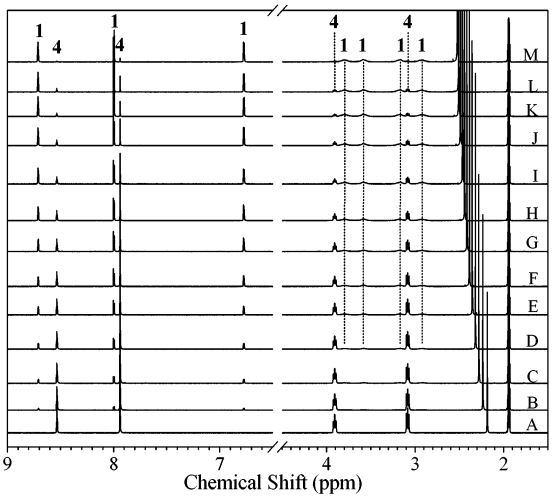

Figure 5. ^{1}H NMR titration of $[Ca(Tatren)(OH_2)]^{2+}$ (**4**) in CD_3CN with $Zn(ClO_4)_2$ in CD_3OD. $[Zn^{2+}]:[Ca^{2+}] = 0$ (A), 0.15 (B), 0.23 (C), 0.31 (D), 0.38 (E), 0.46 (F), 0.54 (G), 0.62 (H), 0.69 (I), 0.77 (J), 0.85 (K), 0.92 (L), and 1.00 (M). The top spectrum is identical with that of authentic $[Zn(Tatren)]^{2+}(ClO_4)_2$ in CD_3CN. The initial concentration of $[Ca(Tatren)(OH_2)]^{2+}$ was 8.17×10^{-3} M. The shifting resonance between 2 and 3 ppm is residual water.

Because the extracellular Ca^{2+} concentration is relatively high, it is possible that Tatren would exist in blood serum as a Ca^{2+} complex. Thus, feasibility as an MMP inhibitor is likely to require displacement of Ca^{2+} from **4** by the target metal ion, Zn^{2+}. The trans-metalation reaction was investigated by titrating $[Ca(Tatren)(OH_2)]^{2+}$ (**4**) with Zn^{2+} (as $Zn(ClO_4)_2$) and tracking the reaction by ^{1}H NMR spectroscopy in CH_3CN. The spectra are shown in Figure 5 and reveal that Ca^{2+} is displaced by 1 equiv of Zn^{2+} in a nearly quantitative fashion. Although formation of a hexacoordinate Zn^{2+} complex is not a structurally accurate model for formation of an inhibited MMP, this result shows proof of concept that the stable $[Ca(Tatren)(OH_2)]^{2+}$ complex can relinquish its chelating ligand in a kinetically facile manner to form a more stable complex. Therefore, alkaline-earth complexes similar to **4** could play a role in distribution and delivery of chelating inhibitors such as Tatren.

Modeling of the Tripodal Ligand. To develop a structural understanding of how tripodal ligands might interact with the MMP active site and to get an estimate of the binding free energy for Tatren, molecular mechanics-based docking calculations were performed as described in the Experimental Section. The active site regions of the MMP catalytic domains are highly conserved and, in addition to the catalytic zinc center, comprise a number of hydrophillic and hydrophobic sites accessible to low molecular-weight inhibitors that coordinate to the Zn^{2+}. These sites line the substrate binding cleft of the catalytic domains on both sides of the zinc and have been designated Sn and Sn', where $n = 1$, 2, or 3.[1a,4e] These sites are illustrated in Figure 6.

Tatren was docked to the substrate binding clefts of MMPs-2, -3, -9, and -13 containing coordinatively unsaturated catalytic Zn^{2+} centers. For MMP-13 the docked structure with the highest rank, as determined from the original FlexX scoring function,[19] is shown in Figure 7. In this structure one imine N atom of Tatren is coordinated to Zn^{2+}. This monodentate structure is in contrast to the bidentate structure one might predict from the X-ray crystal structure of $[Zn(Tatren)](ClO_4)_2$. As for the rest of the MMP-13 docked structure, a second leg of Tatren is bound in the S1′ pocket while the third is curled back over the top of the catalytic Zn^{2+}. The docked structure predicts several hydrogen bonds between imine nitrogen atoms of Tatren and backbone amide N−H moieties. In particular, there is a strong H-bond between the would-be fifth nitrogen ligand of thiazole and the backbone amide of Ala 188, which is located in the S2 binding site on the β strand that flanks the active site. This H-bond could be a factor in the stabilization of monodentate coordination shown in Figure 7. Docking of Tatren into the MMP-2 and MMP-3 active sites shows similar monodentate coordination. Only MMP-9 has a low-energy docked structure with bidentate Zn coordination. In this bidentate structure the H-bond to Ala 188 is lost, while the other two legs adopt a "scissors" conformation around the loop defining the S1′ pocket and hydrogen bonding to successive backbone amide hydrogens (Tyr 423, Arg 242). The leg not in the S1′ pocket is somewhat solvent exposed.

Since docking is based on a force field approach that does not properly predict the metal coordination environment, we have put the first coordination sphere of Zn^{2+} on firmer theoretical ground by performing DFT (B3LYP) and semi-empirical PM3 calculations on several mono- and bidentate structures. These calculations were performed on a portion of the Tatren-bound active site which includes the catalytic Zn^{2+}, three imidazoles, and one leg of the Tatren ligand, totaling 45 atoms. The PM3 calculations predict the lowest energy structure to be 4-coordinate with the thiazolyl N coordinating to Zn (Figure 8B). The 5-coordinate bidentate structure (Figure 8A) is higher in energy by 2.7 kcal/mol. The PM3 structure that most resembles the lowest energy docked MMP-13 active site (Figure 8C) is 4.1 kcal/mol higher than the PM3 ground state. Since these structures are all close in energy, we carried out higher level DFT calculations to get more accurate energetics and geometries. For the geometry optimizations and force constant calculations we used the B3LYP/6-31G level of theory. At these geometries single point DFT calculations were performed using the double-ζ plus polarization basis set, 6-31G*. In contrast to the PM3 results, the lowest energy DFT structure is five-coordinate as shown in Figure 8A. The first coordination sphere in this structure most closely approximates trigonal bipyramidal with the chelate bite angle being only 74.3°. The average equatorial bond angle is 119.1°, and the angle between axial bonds is 168.2°. This is the mode of coordination seen in the crystal structure of $[Zn(Tatren)](ClO_4)_2$ shown in Figure 1. The four-coordinate structure with the acyclic imine N atom coordinated to Zn (Figure 8C) is 11.1 kcal/mol higher in energy, while the four-coordinate thiazole N-coordinated structure (Figure 8B) is 6.7 kcal/mol higher than the ground state. These two structures have nearly idealized tetrahedral geometries. While it is tempting to draw analogy between the PM3-optimized ground state and the docked MMP-13 structure, the small molecule crystal structures, solution NMR spectra, and high-level DFT

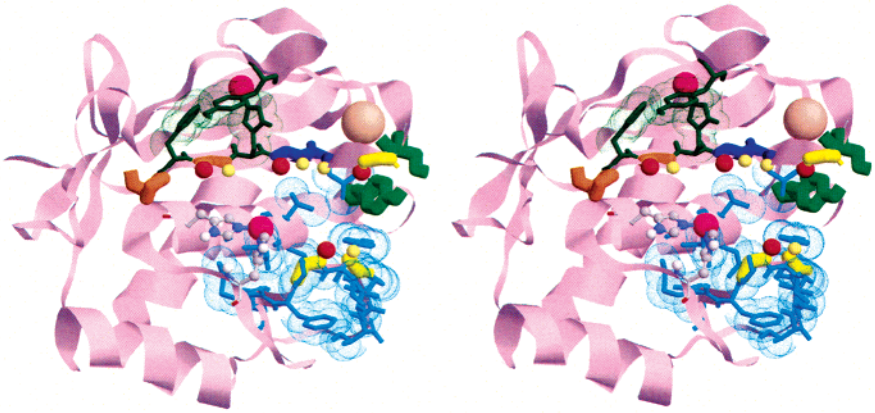

Figure 6. Cross-eyed stereoview of the MMP-13 catalytic domain (PDB code: 830c)[20] showing the subsites for inhibitor binding. Subsite assignments are patterned after refs 1a and 4e. Hydrogen-bonding sites are indicated by spheres with backbone carbonyl oxygen atoms in red and backbone amide hydrogen atoms in ivory. The stippled van der Waals surfaces on the amino acid side chains indicate hydrophobic subsites. The large tan sphere is the structural Ca^{2+} ion, and the slightly smaller pink spheres are the structural (top) and catalytic (center) Zn^{2+} ions. The binding subsites are S1 (blue), S2 (orange), S3 (dark green), S1′ (cyan), S2′ (yellow), and S3′ (light green).

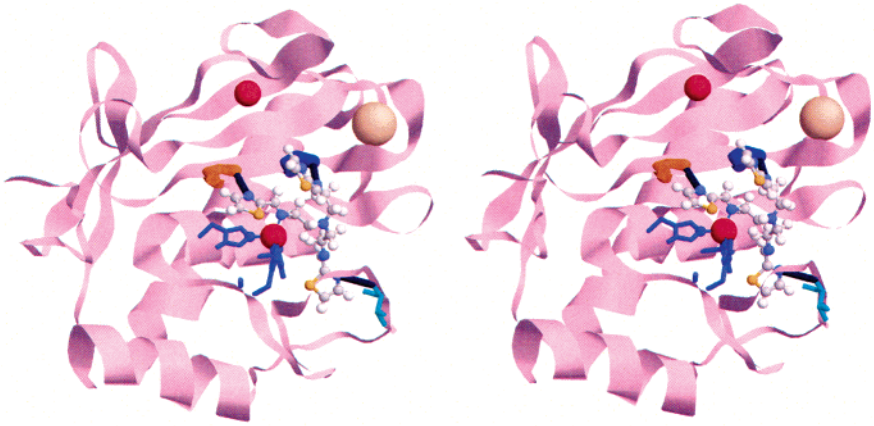

Figure 7. Cross-eyed stereoview of Tatren (ball-and-stick) docked into the active site of the MMP-13 catalytic domain (PDB code: 830c).[20] The catalytic Zn^{2+} center is 4-coordinate with three His imidazole groups (near center of structure) and the acyclic imine N from one leg of Tatren coordinated. The thiazolyl N atom of the coordinating leg is H-bonded to the NH of Ala188 in the S2 subsite. Another leg is inserted into the hydrophobic pocket (formed by the loop at the bottom right of the structure) of the S1′ subsite where the thiazolyl N atom is H-bonded to a backbone NH of Thr245. The third leg is H-bonded through its acyclic imine N atom to the backbone NH of Ala186 in the S1 subsite. Hydrogen bonds between Tatren and backbone amide NH donors are shown as heavy blue lines.

calculations reported here are compelling in their suggestion that a single leg of Tatren is driven to *chelate* the metal center. It is noteworthy that, in addition to giving different ground-state structures, the PM3 method underestimates the energy separations in Figure 8.

Coordination Mode of Tatren in Inhibited MMPs. The most common mode of competitive MMP inhibition by synthetic inhibitors involves coordination of the inhibitor to the catalytic Zn^{2+} ion in the active site.[1] The coordination chemistry of Tatren with Zn^{2+} and Ca^{2+}, the docking results, and DFT calculations presented above suggest that Tatren could be an effective competitive inhibitor of MMPs by virtue of its ability to coordinate to Zn^{2+}. Coordination of more than one leg of Tatren to the catalytic Zn^{2+} ion is considered unlikely due to the steric constrains in the protein active site. This is supported by the docked structures, which suggest formation of a four-coordinate catalytic Zn^{2+} center in the MMP active site. Consistent with the Zn−N bond lengths in **1**, coordination of the acyclic imine N atom is preferred over the thiazoly N (Figure S5A) in the 5-coordinate inhibited enzymes. This structure appears to be further stabilized by a hydrogen bond between the thiazolyl N and a backbone amide NH group in the S3 binding site. However, bidentate chelation of Zn^{2+} by the acyclic imine and thiazolyl N atoms of one leg is also possible, as suggested from the calculated structure of Tatren docked into the MMP-2 active site (Figure S5B). Since these structures are close in energy and the enzyme is held rigid throughout the docking calculation, it is difficult to predict which mode is most important in inhibition.

Inhibition of MMP-13 by Tatren. Much of the impetus for this work is based on the hypothesis that tren-based tripodal ligands have the necessary topology to be competitive active-site inhibitors of matrix metalloproteinases. The computational and experimental results presented thus far clearly show that Tatren chelates 2+ transition metal ions and fits into the substrate binding cleft of MMPs 3, 9, and 13. Thus inhibition of the MMP-13 catalytic domain by Tatren was investigated enzymatically.[18] On the basis of the [Tatren] dependence of the initial rate of substrate hydrolysis, the inhibition constant, K_i, was determined to be 3.5 ± 0.6 μM and inhibition was competitive. Representative kinetic

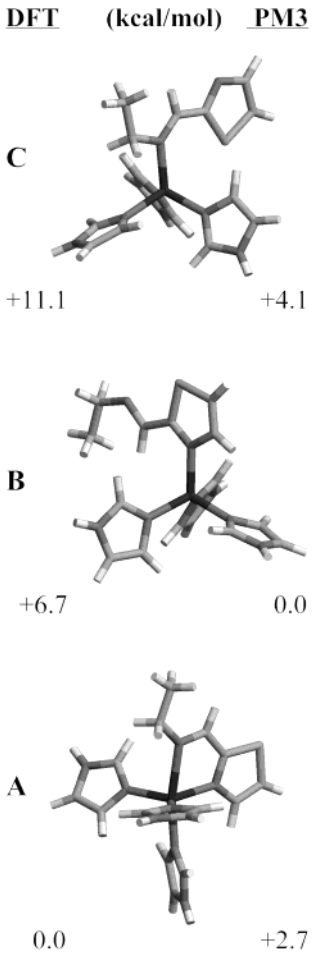

Figure 8. Lowest energy calculated structures of complexes between one leg of Tatren and the MMP active-site model, $[Zn(ImH)_3]^{2+}$. (A) shows the lowest energy binding mode as calculated by DFT, and (B) is the lowest energy binding mode calculated by the semiempirical method, PM3. Energies are given in kcal·mol^{-1}.

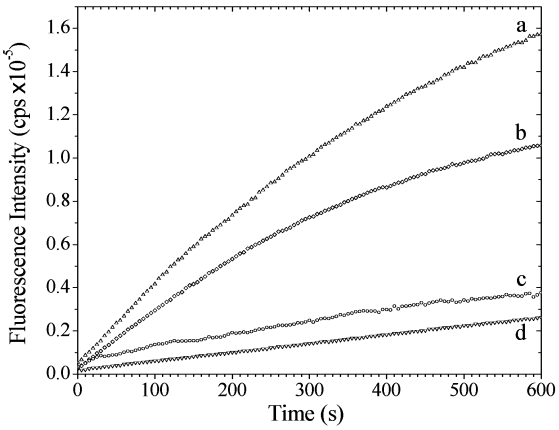

Figure 9. Plot of fluorescence intensity vs time at 393 nm showing inhibition of the MMP-13 catalytic domain by Tatren. [MMP-13] = 15 nM, and [substrate] = 10 μM. [Tatren] = 0 (a), 144 (b), 288 (c), and 577 μM (d).

traces for inhibition of the catalytic domain of MMP-13 are shown in Figure 9. Hence, Tatren is indeed an effective inhibitor of MMP-catalyzed hydrolysis.

For long incubation times of the enzyme with Tatren, the inhibition was largely irreversible. To probe the basis of this irreversibility, we investigated the possibility that Zn^{2+} was being removed from the enzyme. The catalytic domain of MMP-13 (15 nM, 50 μL) and Tatren (10 μM, 10 μL in DMF) were added to 940 μL of buffer, incubated for 2 h, then passed over a Sephadex G25 column. The activity of the enzyme was only 10% of the unincubated control. This inactivated MMP-13 was then treated with Zn^{2+} in buffer for 2 h, after which the excess Zn^{2+} was removed by dialysis. The resulting enzyme was found to have 60% of its original activity, increased 6-fold from its irreversibly inhibited state. Therefore, Tatren appears to remove one or more Zn^{2+} ions from the catalytic domain of MMP-13 over the course of hours under physiological conditions. It should be noted that during the first 15 min of incubation (data collection time for the activity assay), irreversible loss of activity is only 10%, suggesting that inhibition during K_i measurements can be attributed primarily to competitive inhibition. The imine moiety of Tatren is susceptible to slow hydrolysis with a $t_{1/2} \approx 1$ h. It is possible that the irreversible inhibition due to extraction of Zn^{2+} from the enzyme involves tren, which is produced upon hydrolysis of Tatren. We have not attempted to identify the extracted Zn^{2+} complex or evaluate the lifetime of Tatren bound to the MMP active site.

Inhibition of MMP-13 by $[Ca(Tatren)(OH_2)]^{2+}$. Inhibition of the MMP-13 catalytic domain by $[Ca(Tatren)(OH_2)](ClO_4)_2$ was investigated as described above for Tatren. Inhibition was dependent upon $[Ca(Tatren)(OH_2)](ClO_4)_2$ concentration. The inhibition constant, K_i, was determined to be 30 $\pm$ 10 μM, and the concentration dependence of inhibition was consistent with competitive inhibition. This result suggests that Tatren from the Ca^{2+} chelate is available either as the free ligand or as a Ca^{2+} complex to block the MMP-13 active site.

Conclusion. We have shown that catalytic hydrolysis by matrix metalloproteinases can be substantially inhibited by a new and relatively simple tripodal chelating agent, Tatren ($K_i = 3.5$ μM) or by its Ca^{2+} complex ($K_i = 30 \pm 10$ μM). To the best of our knowledge, this is the first such ligand or alkaline-earth chelate to be investigated as MMP inhibitors. Given the simplicity of synthesis and ease with which these compounds can be of modified, they hold promise as design scaffolds for more tightly binding and more enzyme specific MMP inhibitors.

Acknowledgment. The authors wish to thank Dr. Gudrun Lukat-Rodgers and Lei Tang in the Department of Chemistry, North Dakota State University, for their helpful discussions. Thanks are also extended to Mr. Dean Grier for his assistance with the crystallography of **1** and **2**. This work was supported by the NCRR (Grant P20 RR15566).

Supporting Information Available: Crystallographic information files (CIF) for **1**, **2**, **4**, and **5**, Figures S1−S4 showing an ORTEP image of **2**, an ORTEP image of **5**, a spectrophotometric titration of Tatren by Co^{2+}, the Job's plot for isomolar Co^{2+}/Tatren titration, and proposed coordination modes for Tatren with the catalytic zinc center of MMP-13. This material is available free of charge via Internet at http//pubs.acs.org.

IC034811Q